114

SATELLITE & MESOMETEOROLOGY RESEARCH PROJECT

Department of the Geophysical Sciences
The University of Chicago

SATELLITE-TRACKED CUMULUS VELOCITIES

T. Theodore Fujita and Edward W. Pearl
The University of Chicago

and

William E. Shenk
Goddard Space Flight Center

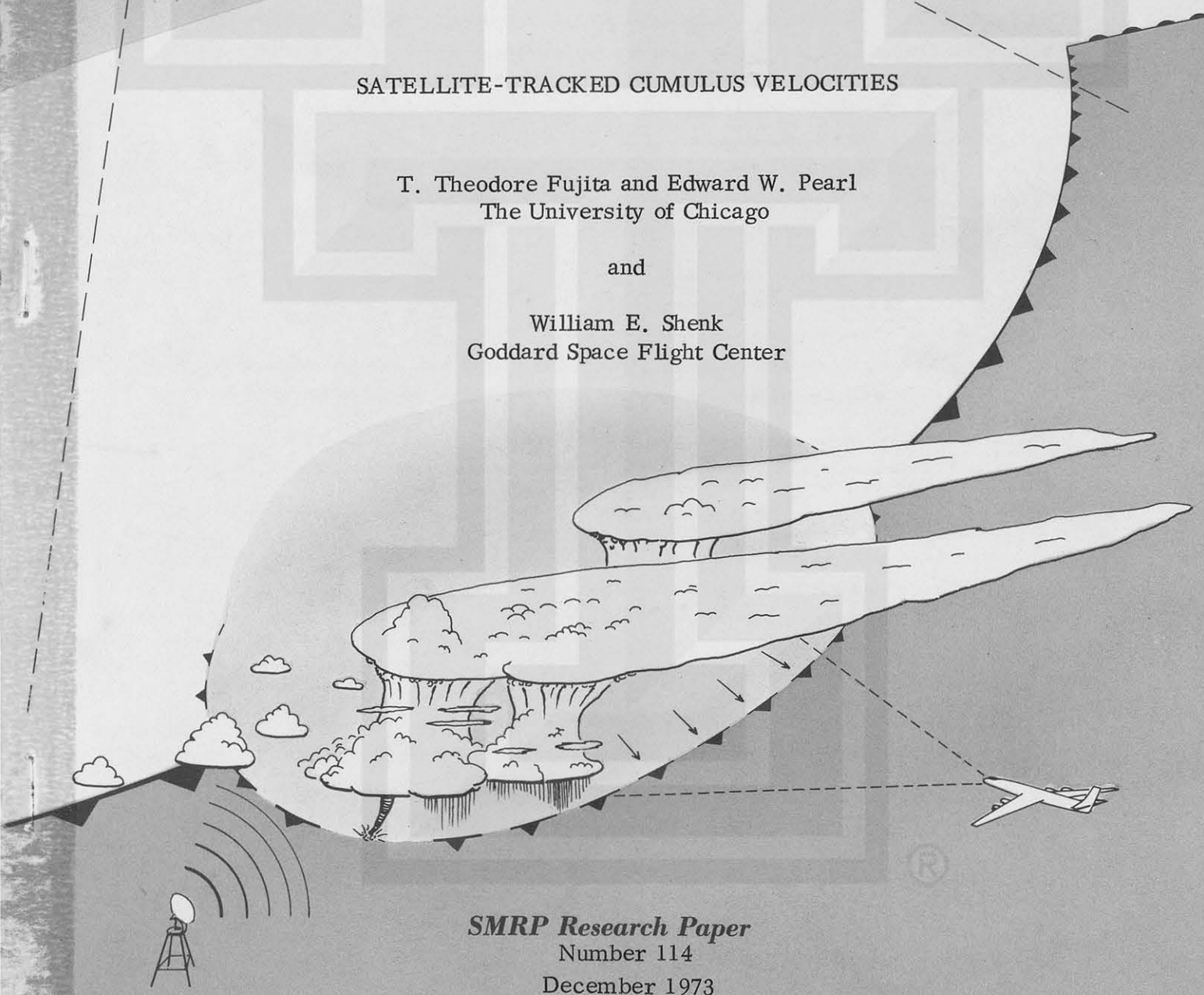

SMRP Research Paper
Number 114
December 1973

MESOMETEOROLOGY PROJECT --- RESEARCH PAPERS

1.* Report on the Chicago Tornado of March 4, 1961 - Rodger A. Brown and Tetsuya Fujita

2.* Index to the NSSP Surface Network - Tetsuya Fujita

3.* Outline of a Technique for Precise Rectification of Satellite Cloud Photographs - Tetsuya Fujita

4.* Horizontal Structure of Mountain Winds - Henry A. Brown

5.* An Investigation of Developmental Processes of the Wake Depression Through Excess Pressure Analysis of Nocturnal Showers - Joseph L. Goldman

6.* Precipitation in the 1960 Flagstaff Mesometeorological Network - Kenneth A. Styber

7.** On a Method of Single- and Dual-Image Photogrammetry of Panoramic Aerial Photographs - Tetsuya Fujita

8. A Review of Researches on Analytical Mesometeorology - Tetsuya Fujita

9.* Meteorological Interpretations of Convective Nephsystems Appearing in TIROS Cloud Photographs - Tetsuya Fujita, Toshimitsu Ushijima, William A. Hass, and George T. Dellert, Jr.

10.* Study of the Development of Prefrontal Squall-Systems Using NSSP Network Data - Joseph L. Goldman

11. Analysis of Selected Aircraft Data from NSSP Operation, 1962 - Tetsuya Fujita

12. Study of a Long Condensation Trail Photographed by TIROS I - Toshimitsu Ushijima

13. A Technique for Precise Analysis of Satellite Data; Volume I - Photogrammetry (Published as MSL Report No. 14) - Tetsuya Fujita

14. Investigation of a Summer Jet Stream Using TIROS and Aerological Data - Kozo Ninomiya

15. Outline of a Theory and Examples for Precise Analysis of Satellite Radiation Data - Tetsuya Fujita

16. Preliminary Result of Analysis of the Cumulonimbus Cloud of April 21, 1961 - Tetsuya Fujita and James Arnold

17. A Technique for Precise Analysis of Satellite Photographs - Tetsuya Fujita

18.* Evaluation of Limb Darkening from TIROS III Radiation Data - S.H.H. Larsen, Tetsuya Fujita, and W.L. Fletcher

19. Synoptic Interpretation of TIROS III Measurements of Infrared Radiation - Finn Pedersen and Tetsuya Fujita

20.* TIROS III Measurements of Terrestrial Radiation and Reflected and Scattered Solar Radiation - S.H.H. Larsen, Tetsuya Fujita, and W.L. Fletcher

21. On the Low-level Structure of a Squall Line - Henry A. Brown

22.* Thunderstorms and the Low-level Jet - William D. Bonner

23.* The Mesoanalysis of an Organized Convective System - Henry A. Brown

24. Preliminary Radar and Photogrammetric Study of the Illinois Tornadoes of April 17 and 22, 1963 - Joseph L. Goldman and Tetsuya Fujita

25. Use of TIROS Pictures for Studies of the Internal Structure of Tropical Storms - Tetsuya Fujita with Rectified Pictures from TIROS I Orbit 125, R/O 128 - Toshimitsu Ushijima

26. An Experiment in the Determination of Geostrophic and Isallobaric Winds from NSSP Pressure Data - William Bonner

27. Proposed Mechanism of Hook Echo Formation - Tetsuya Fujita with a Preliminary Mesosynoptic Analysis of Tornado Cyclone Case of May 26, 1963 - Tetsuya Fujita and Robbi Stuhmer

28. The Decaying Stage of Hurricane Anna of July 1961 as Portrayed by TIROS Cloud Photographs and Infrared Radiation from the Top of the Storm - Tetsuya Fujita and James Arnold

29. A Technique for Precise Analysis of Satellite Data, Volume II - Radiation Analysis, Section 6. Fixed-Position Scanning - Tetsuya Fujita

30. Evaluation of Errors in the Graphical Rectification of Satellite Photographs - Tetsuya Fujita

31. Tables of Scan Nadir and Horizontal Angles - William D. Bonner

32. A Simplified Grid Technique for Determining Scan Lines Generated by the TIROS Scanning Radiometer - James E. Arnold

33. A Study of Cumulus Clouds over the Flagstaff Research Network with the Use of U-2 Photographs - Dorothy L. Bradbury and Tetsuya Fujita

34. The Scanning Printer and Its Application to Detailed Analysis of Satellite Radiation Data - Tetsuya Fujita

35. Synoptic Study of Cold Air Outbreak over the Mediterranean using Satellite Photographs and Radiation Data - Aasmund Rabbe and Tetsuya Fujita

36. Accurate Calibration of Doppler Winds for their use in the Computation of Mesoscale Wind Fields - Tetsuya Fujita

37. Proposed Operation of Intrumented Aircraft for Research on Moisture Fronts and Wake Depressions - Tetsuya Fujita and Dorothy L. Bradbury

38. Statistical and Kinematical Properties of the Low-level Jet Stream - William D. Bonner

39. The Illinois Tornadoes of 17 and 22 April 1963 - Joseph L. Goldman

40. Resolution of the Nimbus High Resolution Infrared Radiometer - Tetsuya Fujita and William R. Bandeen

41. On the Determination of the Exchange Coefficients in Convective Clouds - Rodger A. Brown

* Out of Print
** To be published

(Continued on back cover)

ABSTRACT

Velocities of tracer clouds have been computed by NOAA, NASA, Stanford Research, University of Wisconsin, University of Chicago, and others. Despite the fact that their methods and inherent computation speeds are different from each other, the present state-of-art permits the computations with 1 m/sec speed and 4° direction in standard deviation. Such an accuracy in the cloud velocity is satisfactory for most practical purposes.

The research presented in this paper warns that we have to exercise extreme caution in converting cloud velocities into winds. The motion of fair-weather cumuli obtained by tracking their shadows over Springfield, Missouri revealed that the standard deviation in the individual cloud motion is several times the tracking error. The motion of over-ocean cumuli near Barbados clearly indicated the complicated nature of cumulus velocities. Analysis of whole-sky images obtained near Tampa, Florida failed to show significant continuity and stability of cumulus plumes, less than 0.3 mile in diameter.

Cumulus turrets with 0.3 to 2 mile in size appear to be the best target to infer the mean wind within the subcloud layers. Cumulus or stratocumulus cells consisting of x number of turrets do not always move with wind. The addition and deletion of turrets belonging to a specific cell appear to be the cause of the erratic motion of a tracer cell. It may be concluded that the accuracy of wind estimates is unlikely to be better than 2 m/sec unless the physical and dynamical characteristics of cumulus motion is further investigated.

---

[1]The research reported in this paper was performed both at the University of Chicago and at Goddard Space Flight Center. The former was supported by the National Oceanic and Atmospheric Administration, MSL, under grant E-198-68G and by the National Aeronautics and Space Administration under grant NGR 14-001-008. Research on tropical cumuli off Barbados was supported by the Atmospheric Sciences Section, National Science Foundation, NSF Grant GA-31589.

1. Introduction

Since 1968, when ATS pictures became available, meteorologists have been computing cloud velocities, assuming that they can be approximated as environmental winds. Namely, clouds are regarded as natural tracers to infer winds. Unfortunately, a cloud does not move precisely with the environmental wind. In many cases, however, we find a suitable level at which the wind velocity coincides, more or less, with the cloud velocity. Based on this approximation, Hubert and Whitney (1971) introduced the level of best fit (LBF) to designate the altitude of the flow which steers a tracer cloud.

The difference between cloud and wind velocities is resulted by the complicated nature of cloud including the vertical wind shear, up- and downdrafts, the characteristics of entrainment as studied by Stommel (1947) and Simpson (1971). Despite such an inevitable complication, a large-scale flow can be established based mainly on the cloud velocity along with the estimated LBF. Serebreny, Brain and Hadfield (1969) concluded that there were no systematic variations in the velocities when clouds of various sizes are tracked. This would imply that clouds of any size may be tracked in estimating flow patterns. By tracking cumulus cells of various sizes in ATS I pictures, Fujita, Watanabe, and Izawa (1969) obtained patterns of low-level flow over the equatorial east Pacific. As has been pointed out by Simpson and Dennis (1972), tropical cumuli over the ocean are good tracers with relatively long life and time continuity.

As a mesoscale application of satellite imagery, Sikdar and Suomi (1972) determined the expansion of cloud boundary in successive ATS pictures. The mesoscale or the cloud-scale divergence obtained was as large as 50×10^{-5} sec^{-1}, proving that an explosive growth is an important feature of tropical clouds.

Following the Line-Island Experiment, Fujita, Murino, et al. (1968) computed motions of tropical clouds near Hawaii. Meanwhile a network of ground cameras was established at the top of Haleakala volcano on Maui. The comparison of satellite-tracked and terrestrial photogrammetric velocities of clouds resulted in serious questions.

Do clouds move with environmental winds?

If not, what is the error expected?

How does the cloud type influence the error?

and many others. Especially when multi-layer clouds and vertical wind shear are involved, these questions cannot be answered easily.

Meanwhile, the need for estimating winds from satellite-tracked cloud velocities is urgent. GARP/GATE requires detailed information of the accuracy and the nature of cloud tracking. Velocities of numerous cumuli over U. S. to be determined from SMS pictures can be used literally as "a million anemometers", if we know how to interpret them.

To meet these requirements the authors attempted to review basic problems on the interpretation of low-cloud velocities. Both high clouds and cumulonimbi also present serious problems in tracking and interpretation. A research on these clouds is being conducted toward its completion into a separate paper.

2. ATS-Tracked Low-Cloud Velocities

Since the METRACOM system of cloud-velocity computation was completed by SMRP, a large number of experimental computations have been made. In view of the GATE/GARP interest, the tropical north Atlantic was selected as being the test area. For METRACOM system, refer to Chang et al. (1973).

In tracking cumulus cells, extremely large cells were avoided because of the suspicion that their motions could seriously be affected by their development and dissipation. Moreover, a large cloud may extend to high levels and thus be affected by vertical wind shear.

For the purpose of tracking cumulus clouds, clouds may be classified into the following six sizes, see Table I.

Table I. Classification of Cumulus Sizes for Tracking Purposes

Horizontal Dimensions in miles	Classification
less than 0.3	plume
0.3 - 2	turret
2 - 5	small cell
5 - 10	medium cell
10 - 50	large cell
larger than 50	giant cell

Because of the resolution of ATS pictures, neither plume nor turret can be tracked. Target clouds for our experiments have been limited to cumulus cells with a 2-mile size or larger. Whenever possible, however, both small and medium cells were chosen as good targets, while avoiding large and giant cells. Over the regions of scattered to overcast cumuli in ATS pictures several target clouds of these sizes can be found within each one-degree square. Therefore, it is common to be able to track 50 to 100 clouds within a 5-degree square.

Presented in Fig. 1 is an example of the cloud-motion charts produced by the METRACOM system. An elliptical area was divided into southwest and northeast areas each approximately 6-degree square. The former includes 83 cloud-motion vectors and the latter, 102. The computed mean direction of the northeast group is 218.1° with a standard deviation of 6.5° (Fig. 2). The mean speed was calculated to be 12.0 m/s with 1.6 m/s standard deviation. The standard deviation of the southwest group is 8.2° which is 26% larger than that of the northeast group. The reason for this difference is the curved flow seen in the southwest area, suggesting that the variation in cloud velocities includes true meteorological characteristics of the flow.

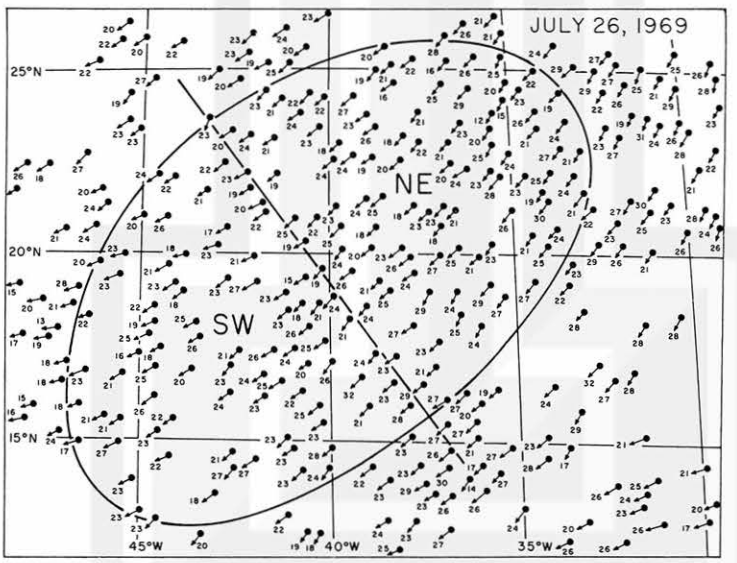

Fig. 1. Low cloud motions extracted from ATS-3 image series in an elliptic area over the tropical North Atlantic. The area was divided into NE and SW portions for statistical analyses. July 26, 1968. The windspeeds are in knots.

The tracking error given by computer, including that of gridding, missynch, etc., appears to be no more than 1.0 m/s standard deviation in the cloud speed. It is conservative to estimate the direction error to be 5°. The cloud tracking with such an accuracy can be achieved as long as we stay within good-target area.

The extreme deviation from the mean speed is 3 to 4 m/s, which is several times larger than the standard deviation. This extreme value is 25 to 30% of the measured cloud speed. The possibility that this extreme was produced by the tracking procedure was assessed. In manual tracking of cumulus cells meteorologists define a tracking point as a position that coincides with the geometric center if a cloud is axially symmetric in both brightness and boundary. However, these cells are hard to find. Instead, what a meteorologist sees is a group of cells in motion. By virtue of pattern recognition, the tracking point of a cumulus cell is selected conveniently at the weighted brightness center. In this test, the meteorologists who performed the tracking were instructed not to follow the geometric center nor the brightness center. In other words, the cloud-motion vector as tracked by the meteorologist is the motion of a cloud of his own definition. We may assume that the extreme variations in the tracked velocities are the results of the nature

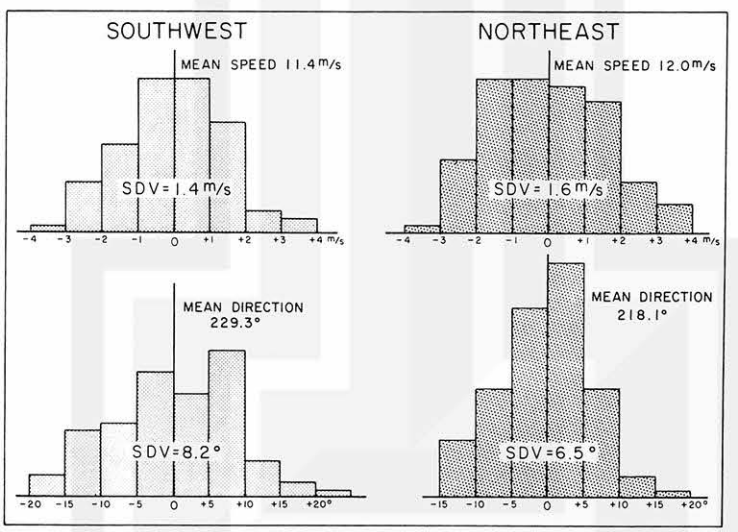

Fig. 2. Distribution of variance in speed and direction of clouds shown in Fig. 1. Standard deviation of 1 m/sec and 5 deg. can be achieved. SDV denotes standard deviation.

of changes in the structure of the tracked cell itself. Some may grow by adding new turrets on a specific side of the cell while others may split into two or more cells, making it very difficult to define the tracking point or points.

3. Problems in Tracking Multi-Turret Cumuli

The size of cumulus and stratocumulus clouds tracked as low-level clouds in the previous section ranges probably between two and ten miles. Much larger clouds were assumed to be bad targets, because a large cloud is likely to be characterized by a large number of tall turrets.

Detailed study of small and medium-sized cells in ATS pictures suggested that cumulus clouds over the tropical Atlantic are very stable compared with their counterparts over the tropical land areas. These clouds over water can be tracked for a period of 30 to 60 minutes without losing their identities as well-defined cells. It should be noted, however, that the shape of a cell varies significantly within the 30 minutes of ATS frame time.

A cumulus cell depicted by a two mile resolution image, for instance, is characterized by

1. Front edge
2. Rear edge
3. Geometric center
4. Brightness center.

Computed cloud velocities may vary according to which of these tracking points is used.

A growing cell tends to move fast when the front edge is tracked. The brightness center, located not always at the geometric center of a cumulus cell is a significant point within a target cloud. Experience shows that the brightness center moves slightly faster than that of the geometric center of the cloud boundary.

A cumulus cell in its dissipating stage is far more complicated in terms of cloud tracking, because a cell does not always shrink into an invisible point. Instead, a cell often splits into two or more pieces, each traveling with a different velocity. Since the split-cell phenomena occur so often, we have not been selecting dissipating cells as being a good target.

During the BOMEX experiment in July 1969, a large number of cumulus pictures were taken at one- to three-minute intervals. The purpose of the photography was to determine the microstructure of cumulus clouds which are to be tracked in GATE/GARP experiments.

A typical example of traveling low-cloud cells is shown in Fig. 3. The sequence was taken at 3-minute intervals in the direction perpendicular to the cloud motion. There are two cells identified, respectively, as a GROWING cell and a DISSIPATING cell.

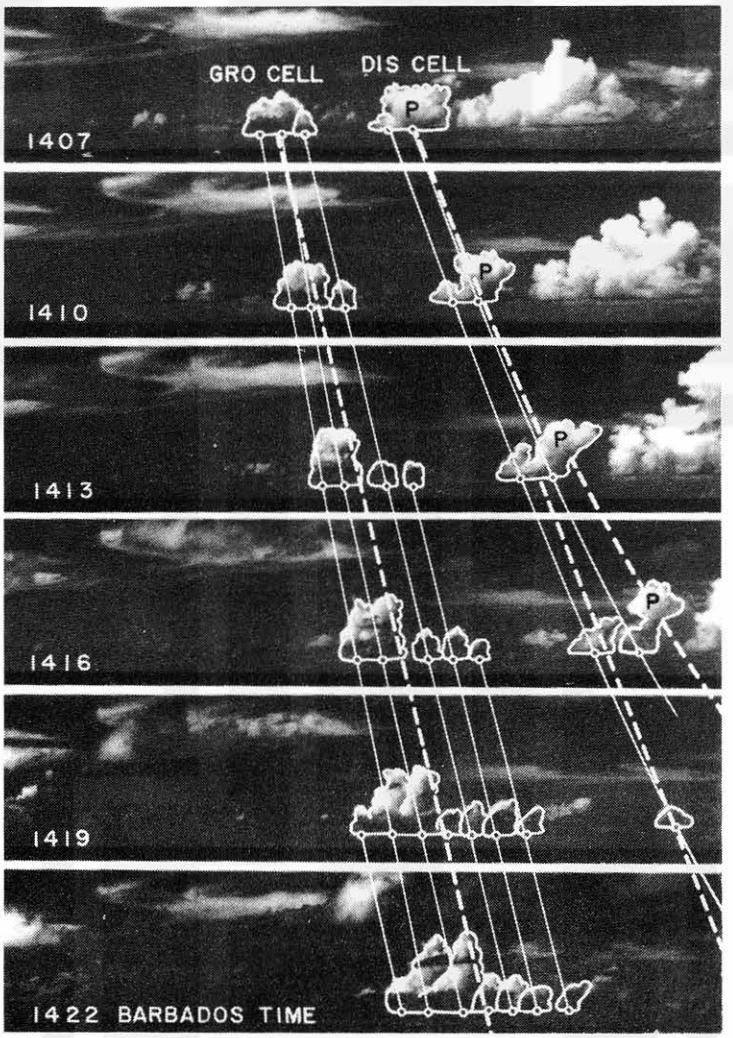

Fig. 3. Horizontal views of multi-turret cumulus cells in their stages of development and dissipation. Taken from Barbados at 3-min intervals facing south. 1407-1422 Barbados time, July 18, 1969.

The growing cell at 1407 was a swelling cumulus approximately 2 miles in size. Within 15 minutes, the cell grew three times into a 6-mile size, consisting of 7 turrets. The center of each turret at the cloud base is identified with a circle. The slope of a line connecting a specific turret is proportional to the horizontal speed of the turret.

Through a simple calculation we are able to estimate the variation of tracked cloud speed as a function of the tracking point, abbreviated as TP.

Table II. Variation of Cloud Speed in Relation to the TP of a 2 to 6 mi size growing cell in Fig. 3

TP	Turret	Front Edge	Rear Edge	Geometric Center	Brightness Center
Rel. Speed	1.00	1.42	0.62	1.16	0.90
% Speed	reference	42% fast	38% slow	16% fast	10% slow

The speed variation shown in Table II is for one case and may not be the representative case of tropical cumuli over the ocean. The table simply points out the importance of the selection of the TP in order to determine the meaningful cloud velocities. The speed variation depends upon various parameters such as growth rate of turrets, preferable location of new turrets, cloud environments including the vertical wind shear, temperature, relative humidity etc.

The dissipating cell in the figure started out with a 2-mile cell, similar to the growing cell to the left. Within several minutes, the cell split into two cells, the one consisting of a weakening turret and the other, a plume ascended from the right-side turret. If we were to track the geometric centers, the speed of each center, before and after the split, is so different that the selection of a proper speed for the dissipating cloud would be impossible.

The plume, P is naturally under the influence of higher-level wind, moving considerably faster than the parent turret. If we are able to estimate the height of the plume based on satellite data, the velocity of the plume can be used effectively for the determination of the vertical wind shear. The purpose of this example and discussion is to point out difficulties in obtaining meaningful cloud velocities by tracking dissipating cells.

The translational velocity of a relatively small turret is likely to represent the mean flow speed within the subcloud layer. Inevitably, there will be some difference between the turret velocity and the mean velocity of the subcloud layer. The difference will depend on the vertical wind shear.

4. 0.3 to 0.5-Mile Resolution

Despite inevitable uncertainties relating cumulus velocities with environmental winds, high resolution satellite pictures are of great value in solving the problems of cloud tracking.

Beginning early in 1974, SMS/GOES will transmit visible pictures with a 0.5-mile resolution. They will provide us with an excellent opportunity for tracking individual turrets rather than their group which appears as a cell in low-resolution pictures.

A DAPP picture of June 19, 1972 showing Lake Michigan and vicinity is presented as an example of one-third mile resolution. The time of the picture is the local noon. Of interest are the cumulus patterns affected by relatively cold lakes, both large and small (see Fig. 4).

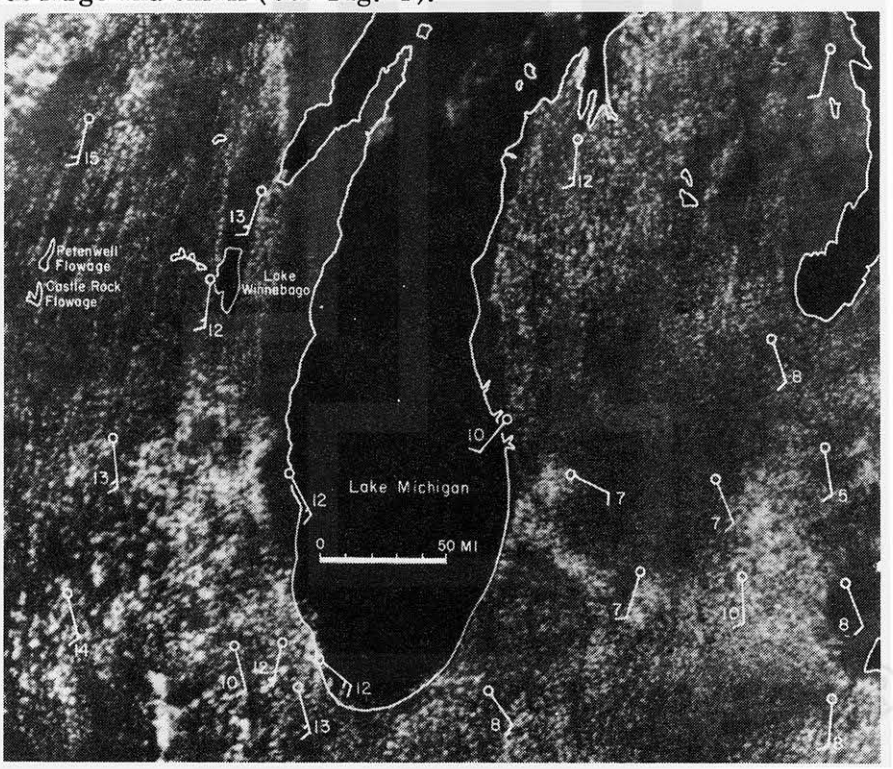

Fig. 4. A DAPP picture with one-third mile resolution showing the Lake Michigan area. 1145 CST June 19, 1972. Surface wind speeds are superimposed.

Wind directions and speeds superimposed upon the DAPP picture reveal the existence of cloud streets over the area with 10 kt or stronger surface winds. The wind field over Lake Michigan is characterized by local divergence, resulting in an extensive cumulus-free area within the wake of the Lake. Even some small lakes in Wisconsin, such as Lake Winnebago and the Petenwell and Castle Rock Flowages are acting as the sources of cumulus-free wakes extending over 50 miles downwind.

If we track the motion of these cumulus cells or turrets in an attempt to determine the environmental winds, it would be feasible to map detailed flow patterns which cannot possibly be determined from surface observations.

ITOS/NOAA satellites have been furnishing us with the Very High Resolution Radiometer (VHRR) pictures with the dual channel of the visible and IR spectra. Estimates of cloud heights have been attempted by combining both IR and visible pictures. An example of a NOAA-2 image enlarged to the resolution limit of the picture is presented in Fig. 5. Numerous cloud streets with both cyclonic and

Fig. 5. VHRR picture of August 2, 1973 enlarged into a full resolution image. The picture was rectified by projecting onto a curved surface.

anticyclonic curvatures are seen over southern Missouri and northern Arkansas. It is of interest to find that no cumulus streets exist beneath scattered fuzzy clouds which are likely to be high clouds. We may speculate that cloud streets formed at this morning hour over cirrus free regions.

In an attempt to determine the density of trackable cumuli a cloud-truth experiment was conducted on April 13-14, 1973. A Learjet was used for the photographic mission, flying over the various regions of cloud formations.

The photograph shown in Figure 6, with 10-mile grid lines superimposed, was taken looking toward Chicago and Gary where a lake-breeze front began to form in the morning. The picture shows that the cloud size varies from 0.1 mile to 2 miles. The number of trackable clouds will naturally vary with the picture resolution.

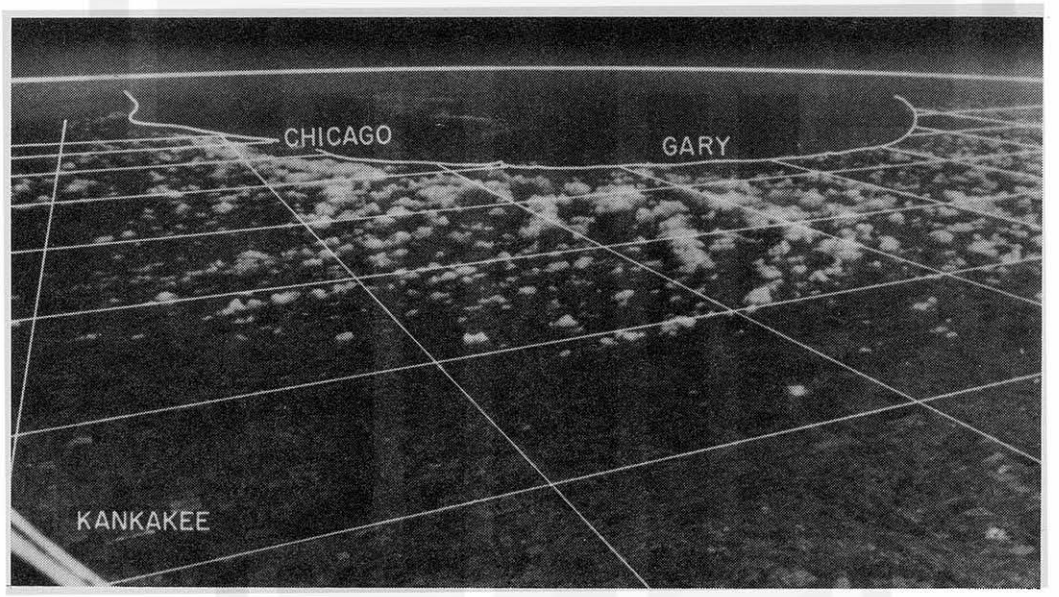

Fig. 6. A view of Chicago and Gary area taken from a Learjet flying at 45,000 ft. showing the development of lake breeze clouds. 0952 CST, April 13, 1973.

If the resolution were 0.5-mile, each square with a 10-mile side would include up to 15 cumuli. The number of trackable clouds within a unit area depends not only upon the picture resolution, but also upon the availability of proper size clouds.

It would be of extreme value to track cumulus clouds in all sizes as soon as SMS/GOES images become available. Such an attempt will permit us to determine the velocities of large clouds in relation to those of surrounding small ones. The motion field of small cumuli could be used to determine the rotational and divergent characteristics of the inflow field around a large cloud.

Do small clouds move with the environmental winds? If the answer is "yes", how small should a trackable cloud be in order to minimize the vector difference between the velocities of cloud and surrounding air? Both encouraging and discouraging answers as to this basic question will be given in the next chapter.

5. Life and Motion of Single Turret Cumuli

For the purpose of photographing small cumuli while looking both upward and downward, a set of whole-sky stereo cameras were operated at the Tampa, Florida airport. The Learjet flights of April 12-13, 1973 were chosen for the time-lapse stereo photography.

Analyses of individual turrets photographed at 5 frames per minute turned out to be rather discouraging because the smaller the clouds the shorter their lives. A half-mile size turret can be tracked for only about 10 minutes. Cloud elements of much smaller size are no more than the condensation particles within the uppermost volume of rapidly changing thermals.

Presented in Fig. 7 is a typical example of a cumulus turret (identified with black dots) and rapidly changing cumulus plumes. The shape and the motion of the plumes, less than 0.3-mile across, are so erratic that variations of 30% in speed and 30° in the direction are commonly observed.

Small pieces of clouds are not moving with the horizontal components of the environmental winds. The addition of the newly condensed droplets due to the thermal-size upward motion as well as the differential evaporation of small droplets contributes significantly to the irregular movement of whole-sky tracked motion of plumes.

Cumulus turrets with 0.3 to 2-mile horizontal dimensions were found to move rather steadily. The cloud with the black dot in Fig. 7 reached a 0.4-mile

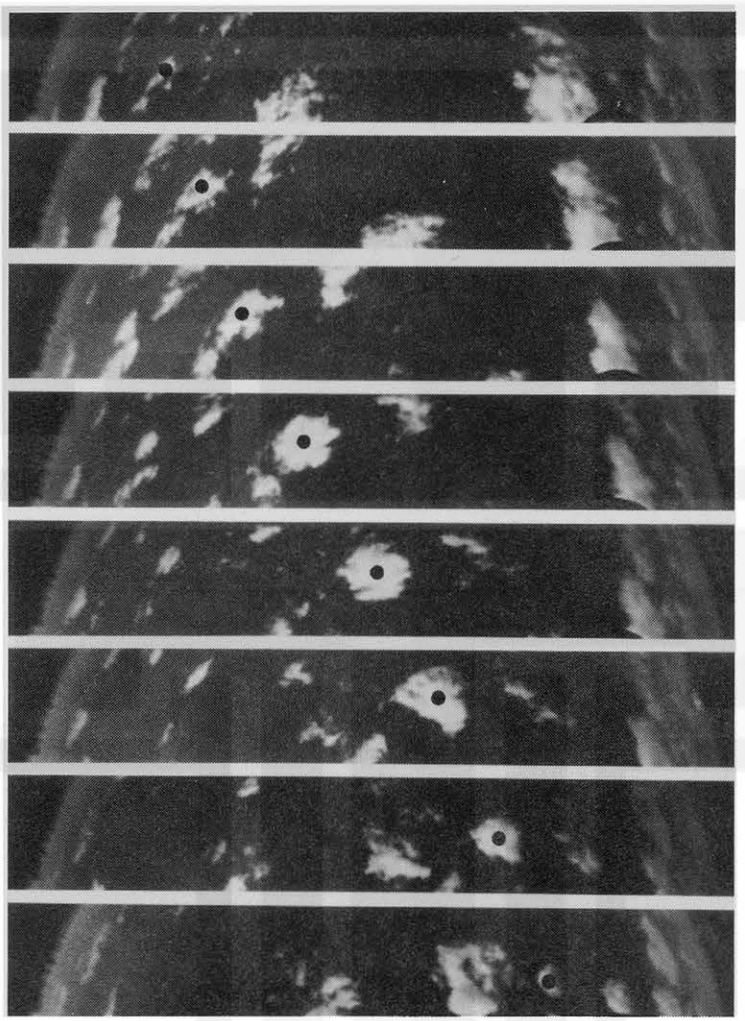

Fig. 7. A cumulus turret as seen in a series of whole-sky pictures taken at one-minute intervals. 1203-1210 EST, April 10, 1973.

size during its 10-minute life across the picture field. It should be noted, however, that a steady motion of cumuli does not mean that their motion coincides with the environmental winds. Nonetheless, a steady motion is more meaningful in terms of its comparison with the environmental winds. In other words, 0.3 to 2-mile size turrets appear to be characterized by relatively steady sub-cloud updrafts. The translational motion of an updraft is closely related to the mean horizontal motion of the subcloud layer in which the root of the updraft is embedded.

In order to determine the motion of single- and dual-turret cumuli, a method of tracking cloud shadows has been developed. Shadow tracking using aerial photographs is very accurate where the shadow movements are related to ground objects on a topographic map. During the tracking period of up to about 10 minutes, the change in the direction of the sun is no more than 3° which may be neglected for most practical purposes.

On May 15, 1972, the day of ATS-III picture shown in Fig. 8, a test experiment of shadow tracking was conducted while flying over Springfield, Missouri. A Learjet flying at 45,000 ft. was used as the platform for this purpose. Springfield was selected for three reasons: the availability of 7-1/2 min. maps covering the metropolitan area, the existence of 0.1 to 2-mile cumuli, and a PIBAL release at 1200 CST about two hours prior to the aircraft flight.

As shown in the ATS picture, Springfield was located in the southwest sector of an occluded low pressure system centered near Detroit, Michigan. The city area was under the influence of the northwesterly flow. Scattered cumuli appearing as a vast gray area extended eastward to the main cloud mass.

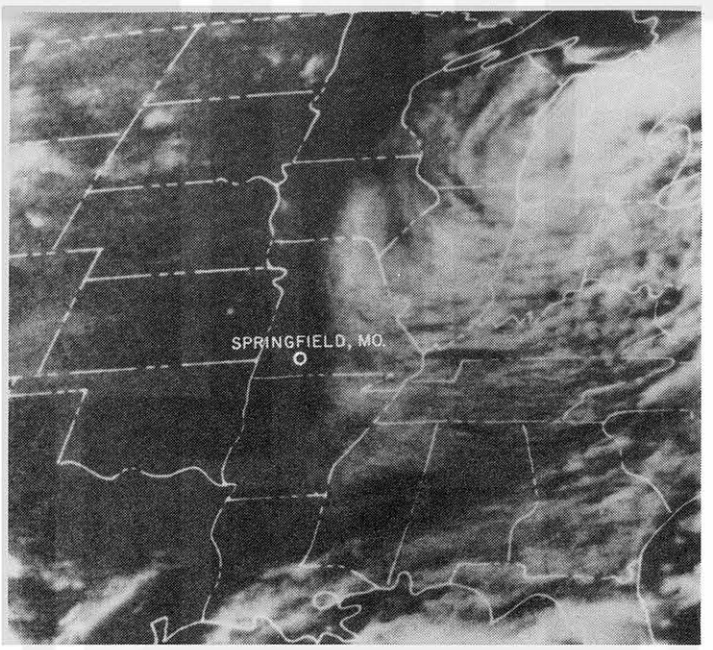

Fig. 8. An ATS picture taken at the time of the cloud shadow experiment. 1249 CST, May 15, 1973.

A series of oblique photographs such as those shown in Fig. 9 were taken every 30 sec on the minute and half minute. Selected target shadows were also photographed with a 135-mm lens at 15 and 45 sec past each minute, so that important shadows can be evaluated at 15-sec intervals.

Fig. 9. An example of the aerial pictures taken over Springfield. Picture time, 1347 CST, May 15, 1973.

An example of the shadow mapping over the city of Springfield is shown in Fig. 10. Geometric centers of shadows at one-minute intervals are given in either large or small circles, depending upon the cloud dimensions. The shadow tracks in the figure appear somewhat like a stretched S shape, revealing that clouds obtained their northwesterly motion as they grew larger.

The major source of error in tracking shadows is not their position inaccuracy. Instead, the determination of the geographic center of the irregular shaped shadow boundary appears to be the problem. The change in the shadow shape becomes more pronounced when a weak thermal produces a tiny cloud. Most of the tracking errors and uncertainties can be minimized through successive fixes at 15 to 30-sec. intervals.

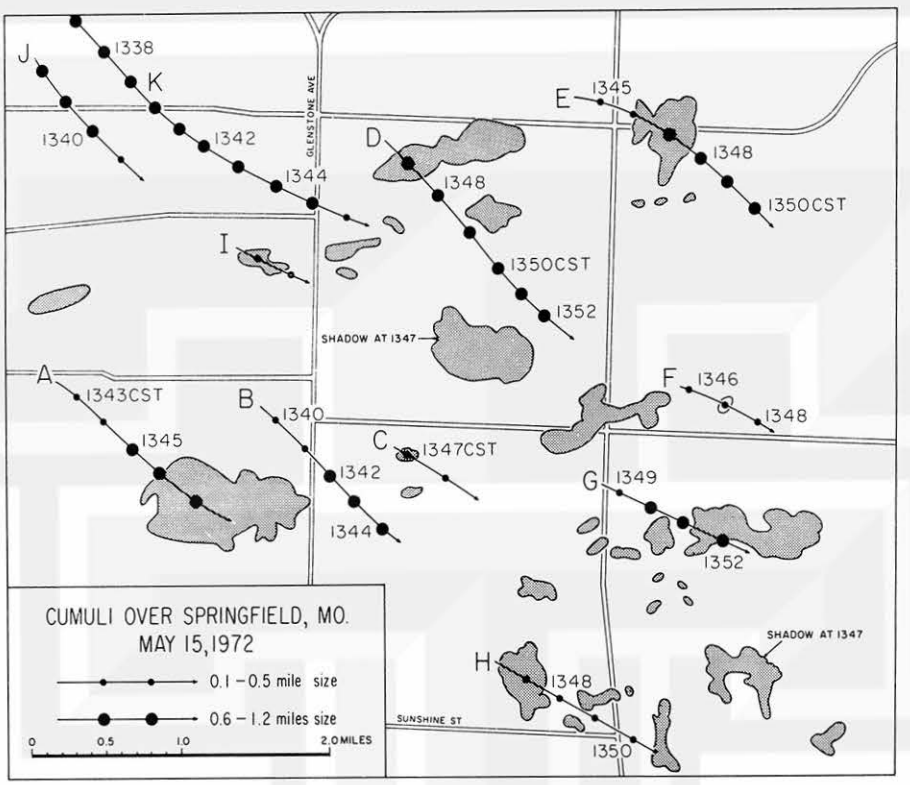

Fig. 10. Tracks of cloud shadows over Springfield. Note that some tracks curve like a stretched letter S.

The S-shaped shadow tracks can be explained based on the 1200 CST PIBAL at Springfield (see Fig. 11). The wind direction below the cloud base at 5,500 ft was about 310°, while the wind direction above the cloud base shifted to 325°. Such a vertical wind shear may curve the trajectory of tall clouds slightly to the right, resulting in a right deviation. When updraft decreases, the newly condensed portion of a cloud will drift, being affected by the mean flow within the subcloud layers. The cloud motion will, then, deviate to the left, thus completing an S-shaped shadow trajectory.

Statistical diagrams of cloud motion give interesting distributions of the direction and speed (see Fig. 12). As for the speed, small clouds tended to move faster than large ones. One contributing factor to this result may be the effective height of the root of the updraft. Since the wind speeds within the subcloud layers increased upward the higher the root of the updraft, the larger the horizontal momen-

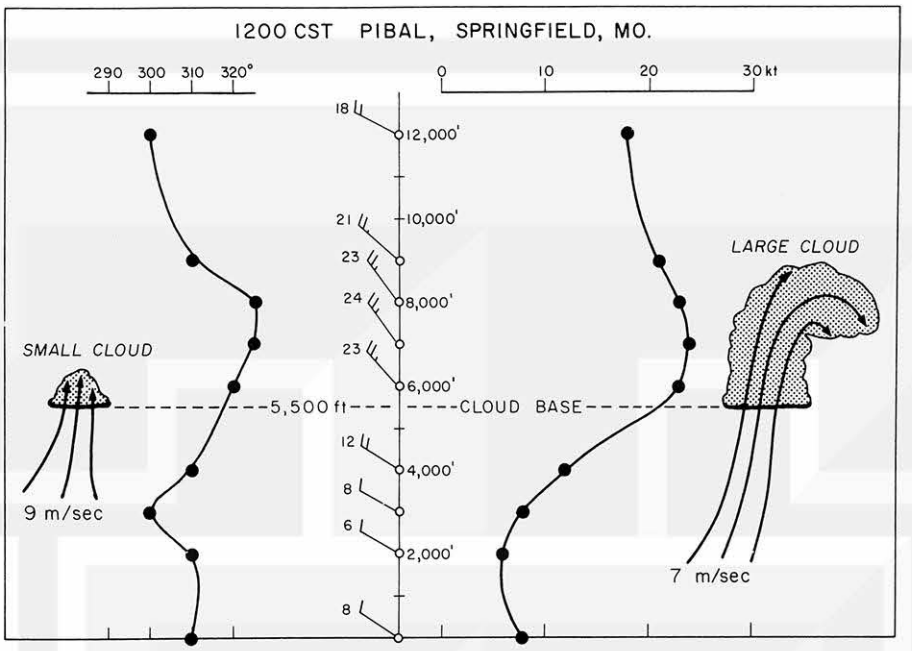

Fig. 11. A model or cumulus clouds used for tracking their shadows over Springfield, Missouri. May 15, 1972.

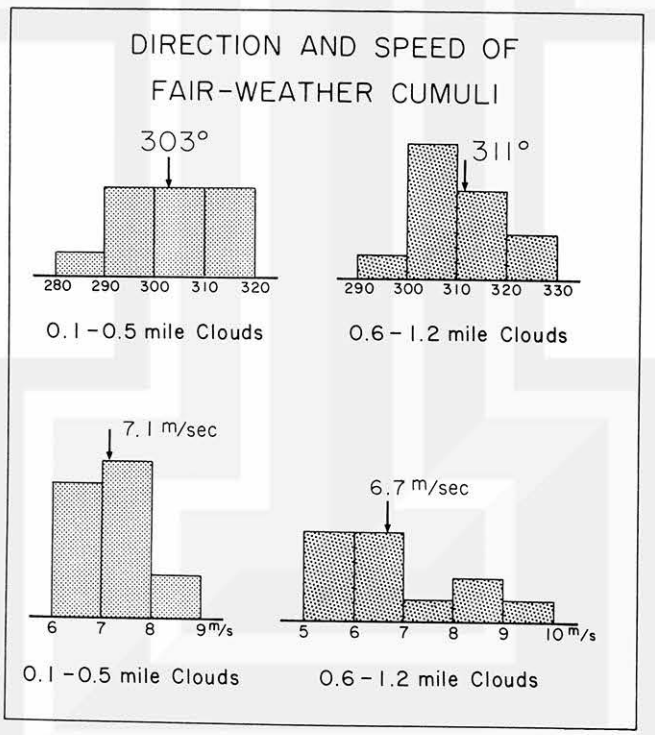

Fig. 12. Direction and speed of fair-weather cumuli over Springfield, Missouri. Motions computed from cloud shadows. May 15, 1972.

tum at the cloud base. If we assume that the effective height of the inflow for a large cloud is much lower than that for a small cloud, a small cloud could move faster than a large one.

The effective height of the inflow is a difficult parameter to define because the entrainment taking place below the cloud base has a tendency to raise the effective height. In effect, a small updraft or a thermal originating near the surface will be mixed with the horizontal wind within the upper subcloud layers due to the overwhelming entrainment. On the other hand, a large cloud will be able to draw the air from the lower subcloud layers without suffering much from the effects of entrainment.

6. Conclusions

Since ATS I and III pictures became available to meteorologists, cloud tracking to infer environmental winds became one of the most important end products. In view of the inherent difference between cloud and air motions, proper interpretation of the tracked cloud velocities in relation to three-dimensional air motion around target clouds is of vital importance.

The nature of the low-cloud velocity explored in this paper revealed that it would be necessary not to interpret cloud velocities as being the environmental winds. The basic knowledge of cloud parameters, involving cloud dynamics, cloud heights, LBF, cloud types, will permit us to minimize the possible error in the wind estimates.

Naturally some target clouds are good, while others are bad. "Cumulus Plumes" less than 0.3 mile in horizontal dimensions are bad targets because of their unsteady updrafts. This would mean that it is not necessary to increase the image resolution beyond about 0.3 mile for the purpose of cumulus tracking.

"Cumulus Turrets" ranging between 0.3 and 2 miles in size are concluded to be the best target to infer winds within the subcloud layers. They are likely to be single-turret clouds. From the tracking point view, however, these clouds are hard-to-track targets, because they are small and relatively short in life.

"Small Cells", 2 to 5 miles in size are also good targets for wind determination. Because of the expected variation of turrets within a cell, a proper tracking point such

as brightness or geometric center will have to be selected. These cells are easy targets to be tracked for up to two hours, especially over the ocean.

"Medium, Large, and Giant Cells" are the easiest target to be tracked. If these cells are relatively flat, somewhat like stratocumulus cells, their motion is not too far from that of small cells. Cells with deep, penetrative convection often move differently, necessitating their discrimination against small cells.

Cumuliform clouds seen over land areas are short lived, characterized often by an erratic motion. Experiences have shown that large turrets and small cells in successive ATS pictures do not always maintain their continuity. These target clouds are, however, very important in estimating the low-level flow over continents. It would be necessary to investigate kinematic characteristics of small cells based on SMS/GOES pictures and cloud-truth experiments.

REFERENCES

Chang, Y.-M., J. J. Tecson, and T. T. Fujita (1973): METRACOM System of Cloud-Velocity Determination from Geostationary Satellite Pictures. SMRP Paper 110, The University of Chicago.

Fujita, T. T., D. L. Bradbury, C. Murino, and L. Hull (1968): A Study of Mesoscale Cloud Motions computed from ATS-I and Terrestrial Photographs. SMRP Paper 71, The University of Chicago. 25 pp

Fujita, T. T., K. Watanabe, and T. Izawa (1969): Formation and Structure of Equatorial Anticyclones Caused by Large-Scale Cross-Equatorial Flows Determined by ATS-I Photographs. J. Appl. Meteor. 8, 649-667.

Hubert, L. F. and L. F. Whitney, Jr. (1971): Wind Estimation from Geostationary Satellite Pictures. Mon. Wea. Rev., 99, 665-672.

Serebreny, S. M., A. E. Brain, and R. G. Hadfield (1969): Comparisons of Measurements of Cloud Motions. Stanford Research Institute Final Report, Contract E-11-69 (N).

Sikdar, D. N. and V. E. Suomi (1972): On the Remote Sensing of Mesoscale Tropical Convection Intensity from a Geostationary Satellite. J. Appl. Meteor. 11, 37-43.

Simpson, J. S. (1971): On Cumulus Entrainment and One-Dimensional Models. Jour. Atmos. Sci., 28, 449-455.

Simpson, J. S. and A. S. Dennis (1972): Cumulus Clouds and their Modification. NOAA Tech. Memo. ERL-OD 14, Boulder.

Stommel, H. (1947): Entraining of Air into a Cumulus Cloud. J. Of Meteor. 4, 91-94.

MESOMETEOROLOGY PROJECT - - - RESEARCH PAPERS

(Continued from front cover)

42.* A Study of Factors Contributing to Dissipation of Energy in a Developing Cumulonimbus - Rodger A. Brown and Tetsuya Fujita

43. A Program for Computer Gridding of Satellite Photographs for Mesoscale Research - William D. Bonner

44. Comparison of Grassland Surface Temperatures Measured by TIROS VII and Airborne Radiometers under Clear Sky and Cirriform Cloud Conditions - Ronald M. Reap

45. Death Valley Temperature Analysis Utilizing Nimbus I Infrared Data and Ground-Based Measurements - Ronald M. Reap and Tetsuya Fujita

46. On the "Thunderstorm-High Controversy" - Rodger A. Brown

47. Application of Precise Fujita Method on Nimbus I Photo Gridding - Lt. Cmd. Ruben Nasta

48. A Proposed Method of Estimating Cloud-top Temperature, Cloud Cover, and Emissivity and Whiteness of Clouds from Short- and Long-wave Radiation Data Obtained by TIROS Scanning Radiometers - T. Fujita and H. Grandoso

49. Aerial Survey of the Palm Sunday Tornadoes of April 11, 1965 - Tetsuya Fujita

50. Early Stage of Tornado Development as Revealed by Satellite Photographs - Tetsuya Fujita

51. Features and Motions of Radar Echoes on Palm Sunday, 1965 - D. L. Bradbury and T. Fujita

52. Stability and Differential Advection Associated with Tornado Development - Tetsuya Fujita and Dorothy L. Bradbury

53. Estimated Wind Speeds of the Palm Sunday Tornadoes - Tetsuya Fujita

54. On the Determination of Exchange Coefficients: Part II - Rotating and Nonrotating Convective Currents - Rodger A. Brown

55. Satellite Meteorological Study of Evaporation and Cloud Formation over the Western Pacific under the Influence of the Winter Monsoon - K. Tsuchiya and T. Fujita

56. A Proposed Mechanism of Snowstorm Mesojet over Japan under the Influence of the Winter Monsoon - T. Fujita and K. Tsuchiya

57. Some Effects of Lake Michigan upon Squall Lines and Summertime Convection - Walter A. Lyons

58. Angular Dependence of Reflection from Stratiform Clouds as Measured by TIROS IV Scanning Radiometers - A. Rabbe

59. Use of Wet-beam Doppler Winds in the Determination of the Vertical Velocity of Raindrops inside Hurricane Rainbands - T. Fujita, P. Black and A. Loesch

60. A Model of Typhoons Accompanied by Inner and Outer Rainbands - Tetsuya Fujita, Tatsuo Izawa., Kazuo Watanabe and Ichiro Imai

61. Three-Dimensional Growth Characteristics of an Orographic Thunderstorm System - Rodger A. Brown

62. Split of a Thunderstorm into Anticyclonic and Cyclonic Storms and their Motion as Determined from Numerical Model Experiments - Tetsuya Fujita and Hector Grandoso

63. Preliminary Investigation of Peripheral Subsidence Associated with Hurricane Outflow - Ronald M. Reap

64. The Time Change of Cloud Features in Hurricane Anna, 1961, from the Easterly Wave Stage to Hurricane Dissipation - James E. Arnold

65. Easterly Wave Activity over Africa and in the Atlantic with a Note on the Intertropical Convergence Zone during Early July 1961 - James E. Arnold

66. Mesoscale Motions in Oceanic Stratus as Revealed by Satellite Data - Walter A. Lyons and Tetsuya Fujita

67. Mesoscale Aspects of Orographic Influences on Flow and Precipitation Patterns - Tetsuya Fujita

68. A Mesometeorological Study of a Subtropical Mesocyclone -Hidetoshi Arakawa, Kazuo Watanabe, Kiyoshi Tsuchiya and Tetsuya Fujita

69. Estimation of Tornado Wind Speed from Characteristic Ground Marks - Tetsuya Fujita, Dorothy L. Bradbury and Peter G. Black

70. Computation of Height and Velocity of Clouds from Dual, Whole-Sky, Time-Lapse Picture Sequences - Dorothy L. Bradbury and Tetsuya Fujita

71. A Study of Mesoscale Cloud Motions Computed from ATS-I and Terrestrial Photographs - Tetsuya Fujita, Dorothy L. Bradbury, Clifford Murino and Louis Hull

72. Aerial Measurement of Radiation Temperatures over Mt. Fuji and Tokyo Areas and Their Application to the Determination of Ground- and Water-Surface Temperatures - Tetsuya Fujita, Gisela Baralt and Kiyoshi Tsuchiya

73. Angular Dependence of Reflected Solar Radiation from Sahara Measured by TIROS VII in a Torquing Maneuver - Rene Mendez.

74. The Control of Summertime Cumuli and Thunderstorms by Lake Michigan During Non-Lake Breeze Conditions - Walter A. Lyons and John W. Wilson

75. Heavy Snow in the Chicago Area as Revealed by Satellite Pictures - James Bunting and Donna Lamb

76. A Model of Typhoons with Outflow and Subsidence Layers - Tatsuo Izawa

* out of print

(continued on outside back cover)

SATELLITE AND MESOMETEOROLOGY RESEARCH PROJECT --- PAPERS
(Continued from inside back cover)

77. Yaw Corrections for Accurate Gridding of Nimbus HRIR Data - Roland A. Madden.

78. Formation and Structure of Equatorial Anticyclones Caused by Large-Scale Cross Equatorial Flows Determined by ATS I Photographs - Tetsuya T. Fujita and Kazuo Watanabe and Tatsuo Izawa.

79. Determination of Mass Outflow from a Thunderstorm Complex Using ATS III Pictures - T. T. Fujita and D. L. Bradbury.

80. Development of a Dry Line as Shown by ATS Cloud Photography and Verified by Radar and Conventional Aerological Data - Dorothy L. Bradbury.

81. Dynamical Analysis of Outflow from Tornado-Producing Thunderstorms as Revealed by ATS III Pictures - K. Ninomiya.

82.** Computation of Cloud Heights from Shadow Positions through Single Image Photogrammetry of Apollo Pictures - T. T. Fujita.

83. Aircraft, Spacecraft, Satellite and Radar Observations of Hurricane Gladys, 1968 - R. Cecil Gentry, Tetsuya T. Fujita and Robert C. Sheets.

84. Basic Problems on Cloud Identification Related to the Design of SMS-GOES Spin Scan Radiometers - Tetsuya T. Fujita.

85. Mesoscale Modification of Synoptic Situations over the Area of Thunderstorms' Development as Revealed by ATS III and Aerological Data - K. Ninomiya.

86. Palm Sunday Tornadoes of April 11, 1965 - T. T. Fujita, Dorothy L. Bradbury and C. F. Van Thullenar (Reprint from Mon. Wea. Rev., 98, 29-69, 1970).

87. Patterns of Equivalent Blackbody Temperature and Reflectance of Model Clouds Computed by Changing Radiometer's Field of View - Jaime J. Tecson.

88. Lubbock Tornadoes of 11 May 1970 - Tetsuya Theodore Fujita.

89. Estimate of Areal Probability of Tornadoes from Inflationary Reporting of Their Frequencies - Tetsuya T. Fujita.

90. Application of ATS III Photographs for Determination of Dust and Cloud Velocities Over Northern Tropical Atlantic - Tetsuya T. Fujita.

91. A Proposed Characterization of Tornadoes and Hurricanes by Area and Intensity - Tetsuya T. Fujita.

92. Estimate of Maximum Wind Speeds of Tornadoes in Three Northwestern States - T. Theodore Fujita.

93. In- and Outflow Field of Hurricane Debbie as Revealed by Echo and Cloud Velocities from Airborne Radar and ATS-III Pictures - T. T. Fujita and P. G. Black (Reprinted from preprint of Radar Meteorology Conference, November 17-20, 1970, Tucson, Arizona).

94. Characterization of 1965 Tornadoes by their Area and Intensity - Jaime J. Tecson.

95.* Computation of Height and Velocity of Clouds over Barbados from a Whole-Sky Camera Network - Richard D. Lyons.

96. The Filling over Land of Hurricane Camille, August 17-18, 1969 - Dorothy L. Bradbury.

97. Tornado Occurrences Related to Overshooting Cloud-Top Heights as Determined from ATS Pictures - T. Theodore Fujita.

98. F P P Tornado Scale and its Applications - T. Theodore Fujita and A. D. Pearson.

99. Preliminary Results of Tornado Watch Experiment 1971 - T. T. Fujita, J. J. Tecson and L. A. Schaal.

100. F-Scale Classification of 1971 Tornadoes - T. Theodore Fujita.

101. Typhoon-Associated Tornadoes in Japan and New Evidence of Suction Vortices in a Tornado near Tokyo - T. Theodore Fujita.

102. Proposed Mechanism of Suction Spots Accompanied by Tornadoes - T. Theodore Fujita.

103. A Climatological Study of Cloud Formation over the Atlantic During Winter Monsoon - H. Shitara

104.** Statistical Analysis of 1971 Tornadoes - Edward W. Pearl.

105. Estimate of Maximum Windspeeds of Tornadoes in Southernmost Rockies - T. Theodore Fujita.

106. Use of ATS Pictures in Hurricane Modification - T. Theodore Fujita.

107. Mesoscale Analysis of Tropical Latin America - T. Theodore Fujita.

108. Tornadoes Around The World - T. Theodore Fujita. (Reprinted from Weatherwise, Vol.26, No. 2, April 1973)

109. A Study of Satellite-Observed Cloud Patterns of Tropical Cyclones - Ekundayo E. Balogun.

110. METRACOM System of Cloud-Velocity Determination from Geostationary Satellite Pictures - Yun-Mei Chang, Jaime J. Tecson and T. Theodore Fujita.

111. Proposed Mechanism of Tornado Formation from Rotating Thunderstorm - T. Theodore Fujita.

112. Joliet Tornado of April 6, 1972 - Edward W. Pearl.

113. Results of F P P Classification of 1971 and 1972 Tornadoes - T. T. Fujita and A. D. Pearson.